

Supplemental Information

Quantitative clonal analysis and single cell transcriptomics reveal division kinetics, hierarchy and fate of oral epithelial progenitor cells

Kyle B. Jones, Sachiko Furukawa, Pauline Marangoni, Hongfang Ma, Henry Pinkard, Rebecca D'Urso, Rapolas Zilionis, Allon M. Klein, and Ophir D. Klein

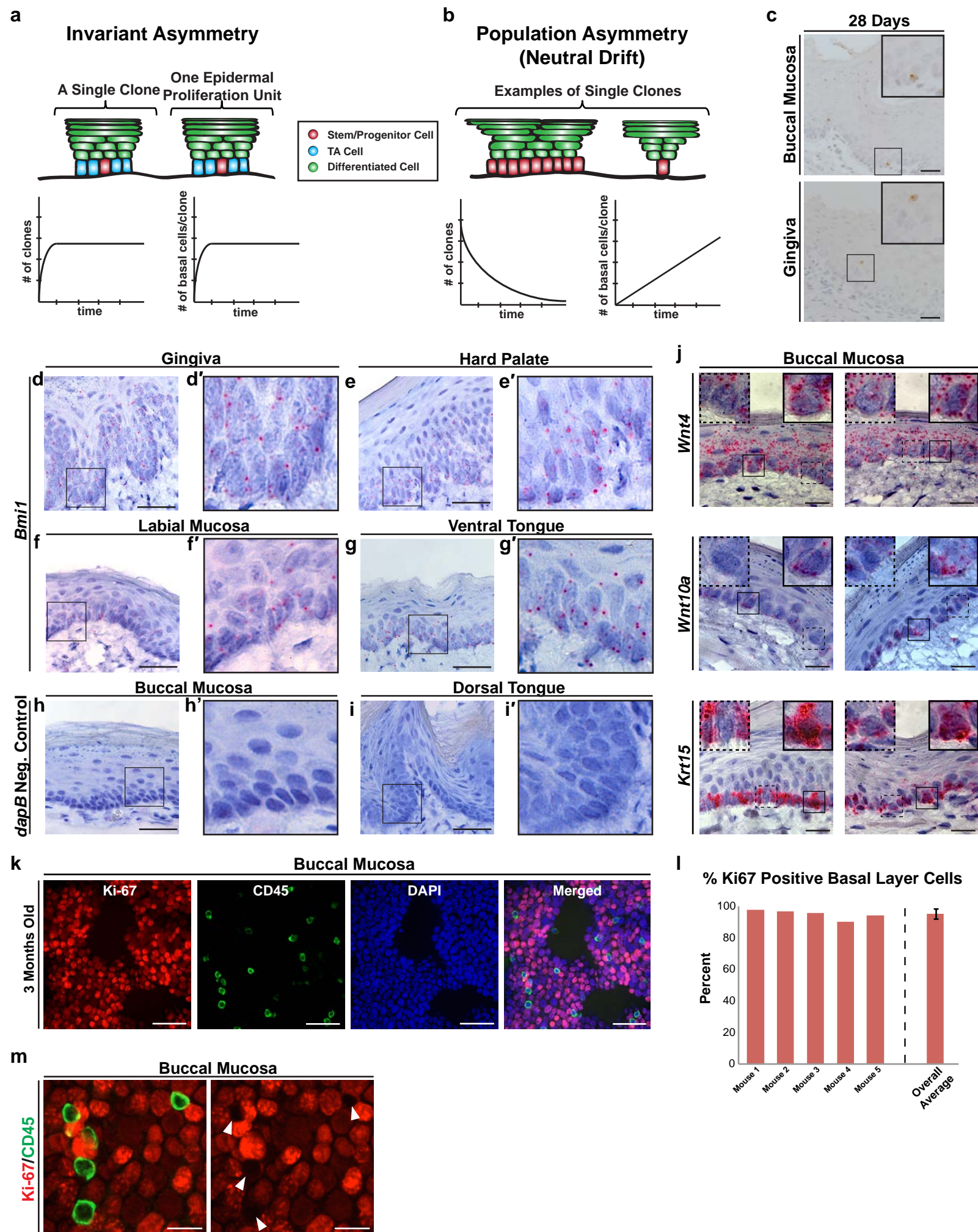
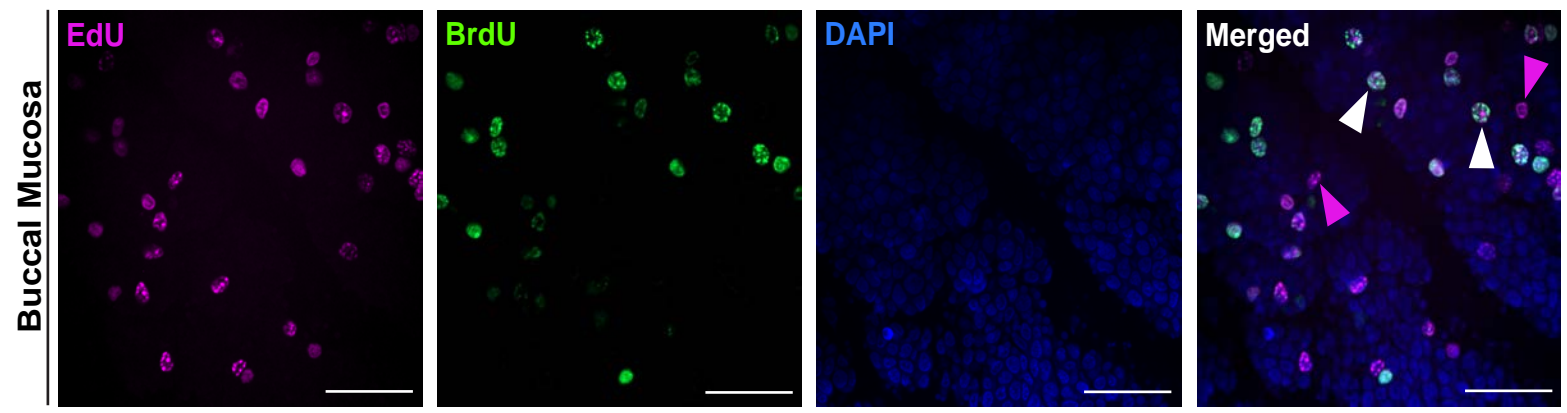
Figure S1

Figure S1. *Bmi1* is expressed predominantly in basal layer keratinocytes throughout the oral mucosa, related to Figure 1. (a,b) Predicted behavior of clones originating from a single, labeled OEPC following invariant asymmetric divisions in the setting of the epidermal proliferation unit model **(a)** or population asymmetric divisions with neutral competition between clones **(b)**. **(c)** Extremely rare BrdU-labeled cells were observed in a seemingly random distribution within the basal and suprabasal layers of the oral mucosa at the 28 day chase. The intensity of the BrdU staining was typically very weak in these cells, indicating that they had undergone mitosis during the 28 day chase and were not completely quiescent. Scale bars, 30 μ m. **(d-i)** Similar to the buccal mucosa and dorsal tongue epithelia, *Bmi1* is also expressed predominantly within the basal layer keratinocytes at other oral mucosal sites (individual *Bmi1* transcripts are represented by red dots). The bacterial gene *dapB* was used as a negative control to assess for background staining and routinely showed no signal **(h,i)**. Scale bars, 30 μ m. **(j)** RNAscope in situ hybridization showing cells with low (dotted line inset image), intermediate, and high (solid line inset image) levels of *Wnt4*, *Wnt10a*, and *Krt15*, confirming the findings from the single cell RNAseq gene enrichment analysis. **(k)** Whole-mount imaging shows that the majority of buccal mucosal basal layer keratinocytes in 10 week old C57BL/6 mice express Ki-67. Scale bars, 30 μ m. **(l)** Bar graphs represent the percentage of basal layer keratinocytes positive for Ki-67 staining along with the overall average \pm SD. **(m)** Although there is a range of Ki-67 staining intensities within basal layer keratinocytes, there is nearly no background staining present as evidenced by the lack of RFP signal in the nuclei of several CD45 positive cells (white arrowheads). This supports

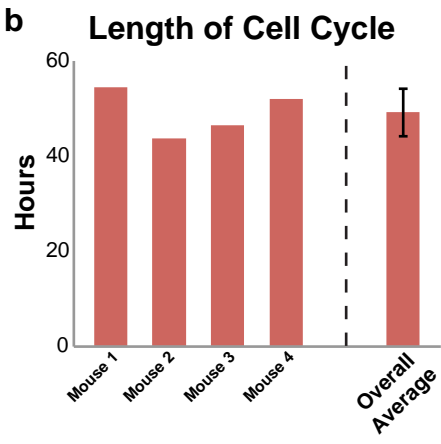
the conclusion that the observed Ki-67 staining is sensitive and specific, albeit faint in some cells. Scale bars, 10 μ m. BrdU, 5-bromo-2'-deoxyuridine.

Figure S2

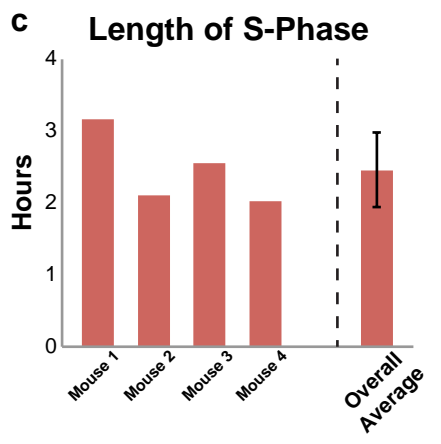
a



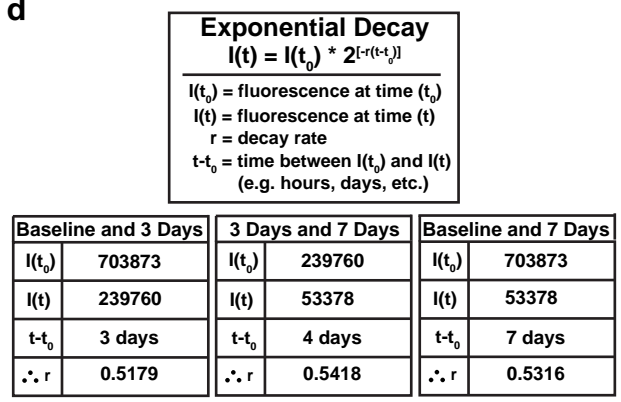
b



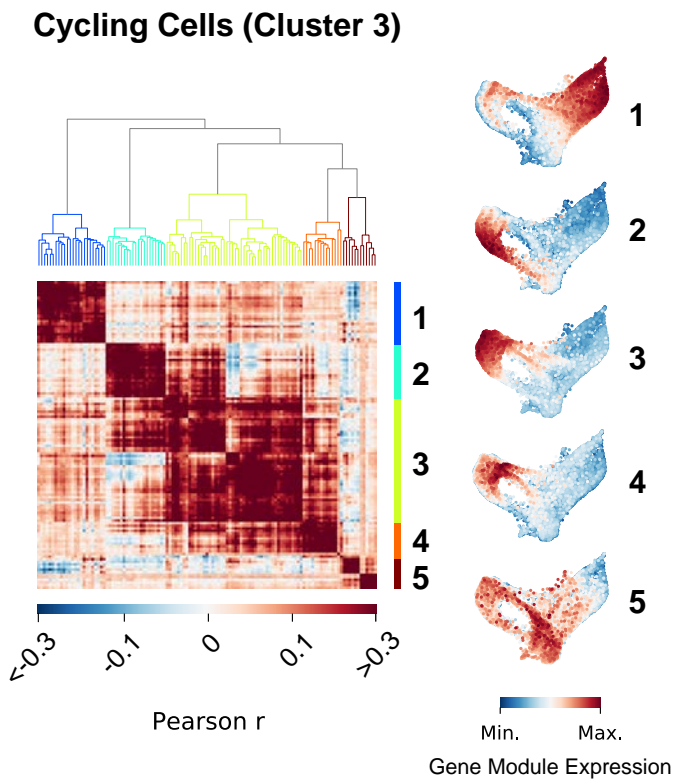
c



d



e



f

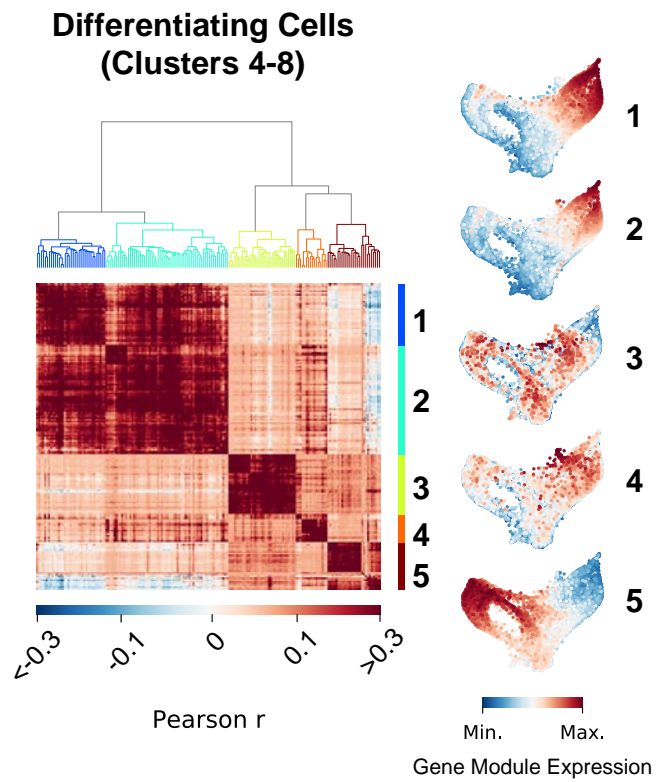


Figure S2. Buccal mucosal basal layer keratinocytes are highly proliferative and exhibit rapid cell turnover, related to Figure 2. (a) Following temporally spaced injections of EdU and BrdU, cells that exit the S-phase prior to euthanasia only label with EdU (pink arrow heads), whereas cells still within the S-phase label with both EdU and BrdU (white arrow heads); see text for further details. Scale bars, 30 μ m. **(b,c)** Bar graphs represent the individual S-phase and total cell cycle times calculated for each of the 8 week old C57BL/6 mice analyzed, along with the overall average \pm SD. **(d)** The exponential decay equation and the decay rate constants calculated from comparisons of different time points in doxycycline treated *K5tTa; tetO-H2B-EGFP* mice. **(e,f)** Positively correlated gene modules identified in oral epithelial cycling cells (cluster 3) and differentiating cells (clusters 4-8). SD, standard deviation; BrdU, 5-bromo-2'-deoxyuridine; EdU, 5-ethynyl-2'-deoxyuridine; DAPI, 4,6-diamidino-2-phenylindole.

Figure S3

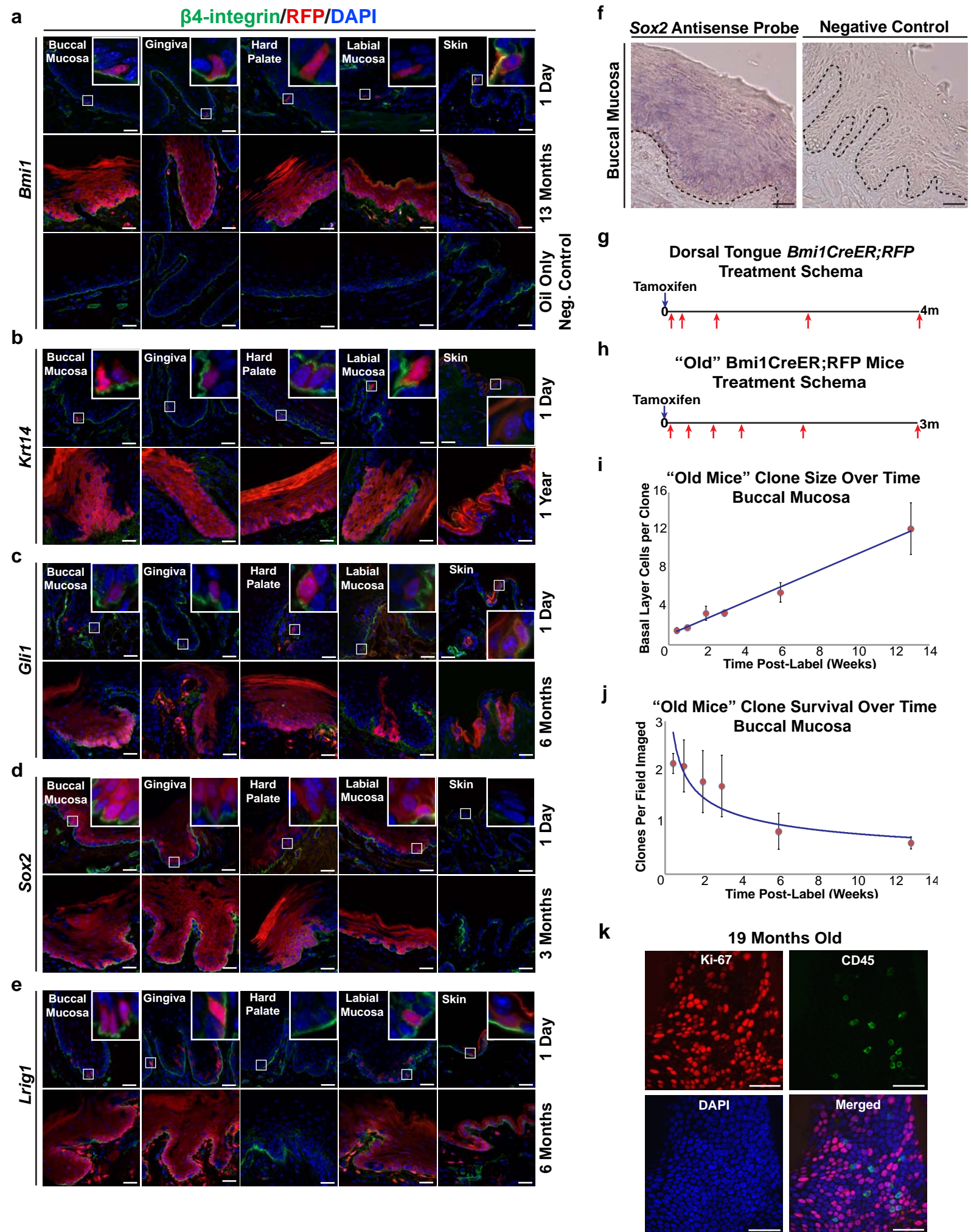


Figure S3. Multiple genes label OEPCs, which follow the population asymmetry model, related to Figure 3. (a) After a single low-dose injection with tamoxifen in *Bmi1^{CreER};R26^{tdTomato}* mice, at the 1 day chase most labeled cells are found in the basal layer. RFP expression is sustained in basal and suprabasal layer keratinocytes for as long as 13 months post-treatment and was almost completely absent in mice that did not receive tamoxifen. Scale bars, 30µm. (b) *Krt14*, a type I keratin intermediate filament, is expressed mainly by basal layer cells in stratified epithelia. After a single low-dose injection with tamoxifen in *K14^{CreER};R26^{tdTomato}* mice, at the 1 day chase most labeled cells are found in the basal layer. RFP expression is sustained in basal and suprabasal layer keratinocytes for as long as 1 year post-treatment. The *K14^{CreER}* construct did exhibit some leakiness (not shown) since areas of RFP expression were observed in mice that did not receive tamoxifen. Scale bars, 30µm. (c) Following activation of the sonic hedgehog (SHH) signaling pathway, *Gli1* translocates to the nucleus and, among other functions, leads to increased transcription of additional *Gli1* mRNA. RFP positivity in cells at early time points post-tamoxifen treatment in *Gli1^{CreER};R26^{tdTomato}* mice indicates that the SHH pathway has been activated in these cells. The SHH pathway plays an integral role during embryonic development as well as in the maintenance of some adult stem/progenitor cell populations under normal homeostatic and repair conditions. After a single low-dose injection with tamoxifen in *Gli1^{CreER};R26^{tdTomato}* mice, at the 1 day chase most labeled cells are found in the basal layer. RFP expression is sustained in basal and suprabasal layer keratinocytes for as long as 6 months post-treatment. The *Gli1^{CreER}* construct did exhibit some leakiness since rare RFP expression was observed in a few mice that did not receive tamoxifen (not shown). Scale bars, 30µm. (d) *Sox2* plays an

integral role in the maintenance of embryonic stem cells in an undifferentiated state and is also expressed within several adult stem cell populations. Following treatment with a single low-dose of tamoxifen in *Sox2^{CreER};R26^{tdTomato}* mice, both basal and suprabasal layer keratinocytes are labeled following a 1 day chase. RFP expression is sustained in basal and suprabasal layer keratinocytes for as long as 3 months post-treatment. *Sox2* expression was not observed in the skin. The *Sox2^{CreER}* construct did exhibit some leakiness since RFP expression was observed in mice that did not receive tamoxifen. Scale bars, 30µm. (e) *Lrig1* is an endogenous late-stage negative regulator of receptor tyrosine kinase signaling. It is also a marker and regulator of various stem/progenitor cell populations in the skin and intestine. After a single low-dose injection with tamoxifen in *Lrig1^{CreER};R26^{tdTomato}* mice, at the 1 day chase most labeled cells are found in the basal layer. RFP expression is sustained in basal and suprabasal layer keratinocytes for as long as 6 months post-treatment. Interestingly, RFP-labeled cells were never detected in the hard palate epithelium; therefore, *Lrig1* does not appear to label OEPCs at this intraoral site. Except for extremely rare instances in the lower lip skin, almost no RFP expression was observed in *Lrig1^{CreER};RFP* mice that did not receive tamoxifen (not shown). Scale bars, 30µm. (f) To confirm the expression pattern of *Sox2* observed in the 1 day chase from (d), in situ hybridization using a *Sox2* antisense probe was performed in the buccal mucosa, which showed generalized *Sox2* mRNA expression in both basal and suprabasal layer keratinocytes. Black dashed lines represent the interface between the connective tissue and epithelium. Scale bars, 30µm. (g) 2-3 month old *Bmi1^{CreER};R26^{tdTomato}* mice were treated with a single dose of tamoxifen, chased at the designated time points, and RFP-labeled clones analyzed in the dorsal tongue epithelium.

(h) 15 month old *Bmi1^{CreER};R26^{tdTomato}* mice were treated with a single dose of tamoxifen, chased at the designated time points, and RFP-labeled clones analyzed. **(i,j)** Similar to clones analyzed in the younger 2-3 month old *Bmi1^{CreER};R26^{tdTomato}* mice, in older mice the number of basal layer keratinocytes per clone increased over time ($0.85 \text{ cells/week} \pm 0.12 \text{ SE}$) while the overall total number of clones decreased ($0.10 \text{ clones/tile/week} \pm 0.02 \text{ SE}$), supporting the population asymmetry model. Solid curves represent predicted neutral drift values. **(k)** Whole-mount imaging of buccal epithelium revealed that on average, older adult mice (19 months old) had fewer basal layer keratinocytes expressing Ki-67 compared with younger mice (3 months old). Scale bars, 30 μm . OEPC, oral epithelial progenitor cell; DAPI, 4,6-diamidino-2-phenylindole; RFP, red fluorescent protein; SE, standard error.

Figure S4

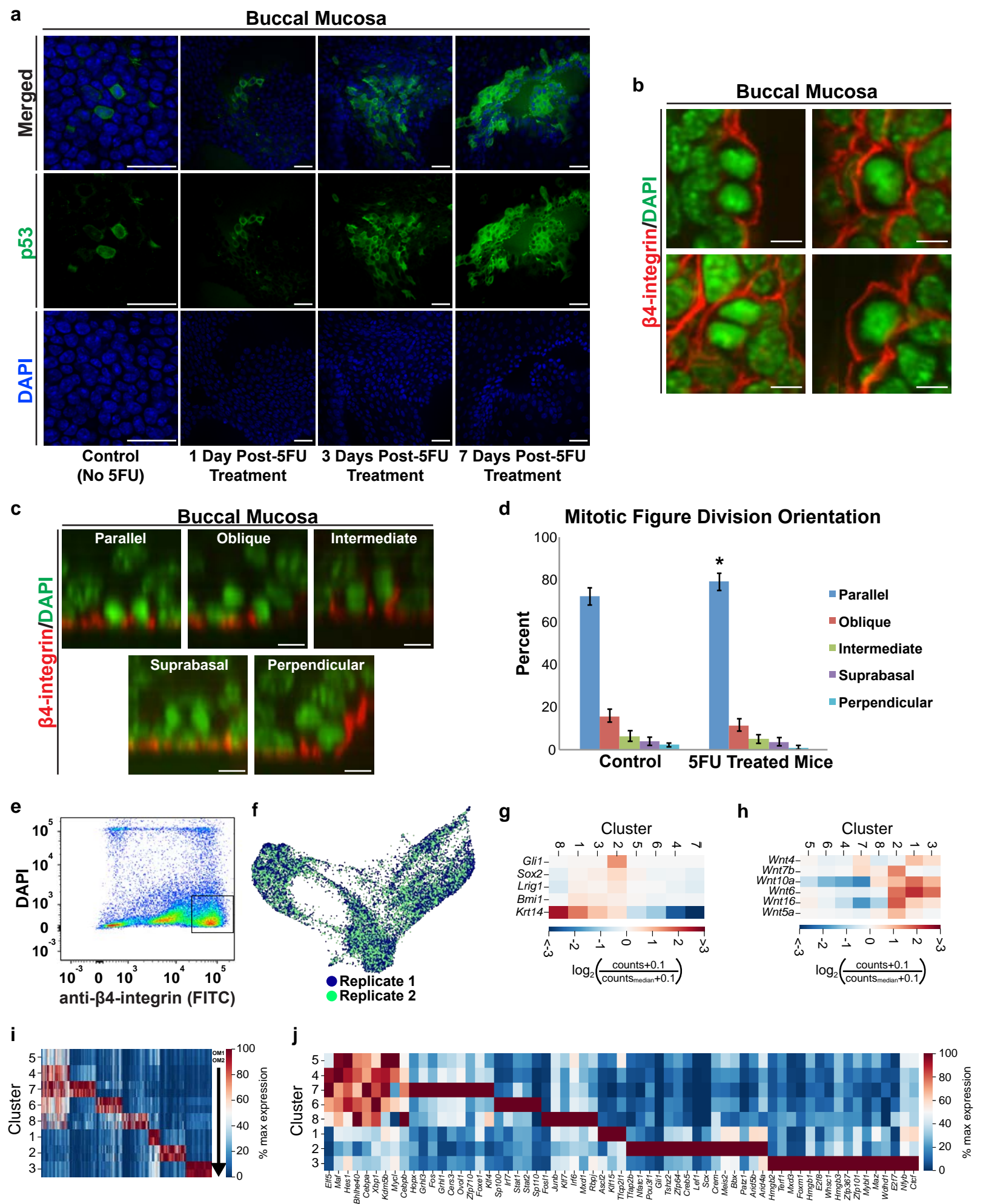


Figure S4. Both p53 expression and parallel oriented mitoses are increased in buccal epithelial basal layer keratinocytes in response to 5FU-induced damage, related to Figure 4. (a) Whole-mount imaging of buccal epithelium from 5FU treated mice reveals progressively increasing levels of cytoplasmic and nuclear p53 protein expression in basal and suprabasal layer keratinocytes. Scale bars, 20 μ m. **(b)** Examples of mitotic figures encountered within the buccal mucosa during analysis. The mitotic figures in the left panels would be suitable for mitotic figure orientation analysis due to clear separation of the sister chromatids, whereas the mitotic figures in the right panels would not be. Scale bars, 5 μ m. **(c)** Reconstructed confocal microscope cross-sections of whole-mount imaged mitotic figures within the buccal epithelium used for mitotic figure orientation analysis. Mitotic figures were grouped into one of 5 categories based on the relationship of the dividing cells to the underlying BM, represented by β 4-integrin, as well as to one another: parallel (both mitotic figures touch the BM), oblique (one mitotic figure touches the BM while the other has lifted off at an approximately 45° angle to the remaining mitotic figure), perpendicular (one mitotic figure touches the BM while the other is directly above the underlying mitotic figure), intermediate (one mitotic figure touches the BM while the second is barely touching the BM and appears to be in the process of lifting off), and suprabasal (both mitotic figures have simultaneously lifted off the BM and are no longer touching it). Scale bars, 5 μ m. **(d)** The vast majority of mitotic figures divide in a parallel orientation with respect to the basement membrane (represented here by β 4-integrin). Following 5FU treatment, there is a small but statistically significant increase in the percentage of parallel oriented mitotic figures (7.1% increase, Fisher's exact test, $p=0.01$). The bar graphs represent the pooled percentage of mitotic figures in each

orientation within control and 5FU treated mice. Error bars represent the 95% confidence interval. **(e)** FACS sorting schema for isolating live, β 4-integrin (CD104) high expressing cells used for single cell RNAseq analysis. **(f)** Technical replicate in the single cell RNAseq analysis show similar distributions across all parts of the SPRING plot. **(g)** mRNA expression patterns of selected stem cell markers in each cluster. **(h)** mRNA expression patterns of selected Wnt genes in each cluster. **(i)** Gene enrichment analysis for each technical replicate (OM1 and OM2) within each cluster. The first column shows enriched genes for clusters 4-8 cumulatively. **(j)** Transcription factor enrichment analysis for each cluster. The left side of the heat map shows enrichment for clusters 4-8 cumulatively. 5FU, 5-fluorouracil; BM, basement membrane; DAPI, 4,6-diamidino-2-phenylindole.